

# Convergence of all-order many-body methods: coupled-cluster study for Li

A. Derevianko,<sup>1</sup> S. G. Porsev,<sup>1,2</sup> and K. Beloy<sup>1</sup>

<sup>1</sup>*Physics Department, University of Nevada, Reno, Nevada 89557, USA*

<sup>2</sup>*Petersburg Nuclear Physics Institute, Gatchina, Leningrad district, 188300, Russia*

(Dated: November 20, 2018)

We present and analyze results of the relativistic coupled-cluster calculation of energies, hyperfine constants, and dipole matrix elements for the  $2s$ ,  $2p_{1/2}$ , and  $2p_{3/2}$  states of Li atom. The calculations are complete through the fourth order of many-body perturbation theory for energies and through the fifth order for matrix elements and subsume certain chains of diagrams in all orders. A nearly complete many-body calculation allows us to draw conclusions on the convergence pattern of the coupled-cluster method. Our analysis suggests that the high-order many-body contributions to energies and matrix elements scale proportionally and provides a quantitative ground for semi-empirical fits of *ab initio* matrix elements to experimental energies.

PACS numbers: 31.15.ac, 31.15.am, 32.10.Fn, 32.70.Cs

Many-body perturbation theory (MBPT) is a ubiquitous tool in atomic and nuclear physics and quantum chemistry. Yet its order-by-order convergence has been found to fail in several systems (see, e.g., [1]). To circumvent this drawback, one usually employs all-order methods which implicitly sum most important classes (chains) of diagrams to all orders of MBPT. Even in this case, as we illustrate here with a nearly-complete solution of the many-body problem for Li, the saturation with respect to a systematic addition of the all-order chains may reveal a non-monotonic convergence. In other words, including increasingly complex (and computationally more expensive) chains does not necessarily translate into a better accuracy.

While such a convergence pattern may seem discouraging, we find that the high-order many-body contributions to energies and matrix elements *vary proportionally* as the all-order formalism is augmented with increasingly complex chains of diagrams. We explain this dependence by the similarity of self-energy contributions to both energies and matrix elements and provide a quantitative ground for semi-empirical fits. This is especially valuable for atomic systems, where high-accuracy experimental data for energies are available, while the matrix elements have a relatively poor accuracy. In some cases, e.g., in parity violation, the matrix elements of the weak interaction are not known experimentally at all, while they need to be computed to a high precision [2, 3]. Although the semi-empirical fits have been used before [3, 4], the validity of such scaling has not been rigorously established. Here, based on a nearly complete many-body calculation, we are able to address this question.

We solve the many-body problem for the three-electron Li atom. Here the availability of both high-accuracy variational Hylleraas and experimental data makes the analysis of minute high-order MBPT effects plausible. Our calculations are complete through the *fourth* order of MBPT for energies and through the *fifth* order for matrix elements. Additionally certain classes of diagrams are summed to all orders using the coupled cluster (CC) method. The previous CC-type formulations for Li [5, 6]

were complete only through the second order for energies and the third order for matrix elements.

We consider Li as a univalent atom and choose the lowest-order Hamiltonian to include the relativistic kinetic energy operator of electrons and their interactions with the nucleus and the  $V^{N-1}$  Dirac-Hartree-Fock (DHF) potential. The single-particle orbitals and energies  $\varepsilon_i$  are found from the set of the frozen-core DHF equations. Using the DHF basis, the Hamiltonian reads (up to an energy offset)

$$H = H_0 + G = \sum_i \varepsilon_i N[a_i^\dagger a_i] + \frac{1}{2} \sum_{ijkl} g_{ijkl} N[a_i^\dagger a_j^\dagger a_l a_k]. \quad (1)$$

Here  $H_0$  is the one-electron lowest-order Hamiltonian,  $G$  is the residual Coulomb interaction,  $a_i^\dagger$  and  $a_i$  are the creation and annihilation operators, and  $N[\dots]$  is the normal product of operators with respect to the core quasivacuum state  $|0_c\rangle$ . Indices  $i, j, k$  and  $l$  range over all possible single-particle orbitals, and  $g_{ijkl}$  are the Coulomb matrix elements.

We are interested in obtaining the exact many-body state  $|\Psi_v\rangle$  that is seeded from the lowest-order DHF state  $|\Psi_v^{(0)}\rangle = a_v^\dagger |0_c\rangle$ :

$$|\Psi_v\rangle = \Omega |\Psi_v^{(0)}\rangle, \quad (2)$$

where  $\Omega$  (yet to be found) is the so-called wave operator [7]. In the CC method the MBPT diagrams are resummed to all orders and one introduces the exponential ansatz for the wave operator

$$\Omega = N[\exp(K)] = 1 + K + \frac{1}{2!} N[K^2] + \dots, \quad (3)$$

where the cluster operator  $K$  is expressed in terms of connected diagrams of the wave operator  $\Omega$ . The operator  $K$  is decomposed into cluster operators  $(K)_n$  combining  $n$  simultaneous excitations of core and valence electrons from the reference state  $|\Psi_v^{(0)}\rangle$  to all orders of MBPT. For

the three-electron Li, the *exact* cluster operator reads

$$K \equiv S_c + D_c + S_v + D_v + T_v = \quad (4)$$

the double-headed arrow representing the valence state.  $S_v$  and  $D_v$  ( $S_c, D_c$ ) are the valence (core) singles and doubles, and  $T_v$  are the valence triples. This exhausts the entire excitation basis for the three-electron Li (e.g., there are no core triples).

In the previous CC work for Li [5] the expansion (4) was truncated at the S and D excitations and the CC equations contained only terms linear in the CC amplitudes (SD method). The full CC study involving S and D excitations was carried out in [8]; we will refer to it as the CCSD approximation. Our present treatment is naturally labeled as CCSDvT to emphasize our additional inclusion of the valence triple excitations.

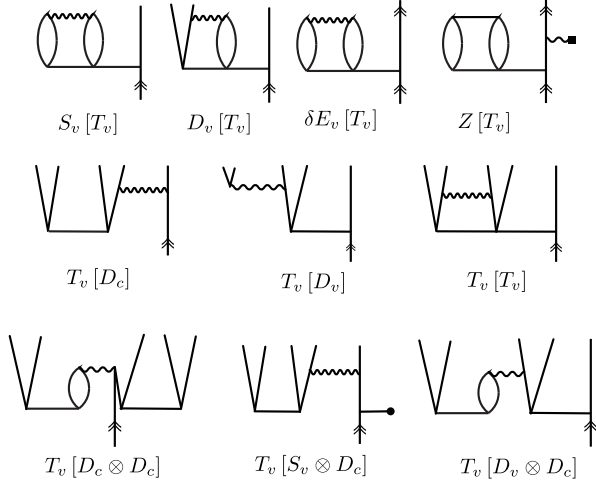


FIG. 1: Representative diagrams for various classes of contributions of the valence triples. The wavy lines represent the residual Coulomb interaction and those capped with the heavy square represent a one-body interaction (e.g., hyperfine interaction).

A set of coupled equations for the cluster operators  $(K)_n$  ( $(K_c)_1 = S_c$ ,  $(K_v)_1 = S_v$ , etc.) may be found from the Bloch equation [7] specialized for univalent systems [9]

$$\begin{aligned} (\varepsilon_v - H_0)(K_c)_n &= \{Q G \Omega\}_{\text{connected}, n}, \\ (\varepsilon_v + \delta E_v - H_0)(K_v)_n &= \{Q G \Omega\}_{\text{connected}, n}, \end{aligned} \quad (5)$$

where the valence correlation energy

$$\delta E_v = \langle \Psi_v^{(0)} | G \Omega | \Psi_v^{(0)} \rangle \quad (6)$$

and  $Q = 1 - |\Psi_v^{(0)}\rangle\langle\Psi_v^{(0)}|$  is the projection operator.

Below we present a topological structure of the CC equations for the cluster amplitudes in the CCSDvT approximation. The resulting equations for the core cluster amplitudes  $S_c$  and  $D_c$  are the same as in the CCSD approximation [10] and we do not repeat them here. Representative diagrams involving triples are shown in Fig. 1. The structure of the valence singles equation is

$$-[H_0, S_v] + \delta E_v S_v = \text{CCSD} + S_v[T_v], \quad (7)$$

where notation like  $S_v[T_v]$  stands for the effect of the valence triples ( $T_v$ ) on the r.h.s. of the equation for valence singles ( $S_v$ ). Here  $[H_0, S_v]$  is a commutator, and  $\delta E_v$  is the valence correlation energy,

$$\delta E_v = \delta E_{\text{CCSD}} + \delta E_v[T_v], \quad (8)$$

where  $\delta E_{\text{CCSD}}$  is obtained within the CCSD approach and  $\delta E_v[T_v]$  is due to the valence triples. The equation for the valence doubles reads

$$-[H_0, D_v] + \delta E_v D_v \approx \text{CCSD} + D_v[T_v].$$

Here we discarded contribution  $D_v[S_c \otimes T_v]$  which stands for a nonlinear contribution resulting from a product of clusters  $S_c$  and  $T_v$ . For the valence triples we obtain

$$\begin{aligned} -[H_0, T_v] + \delta E_v T_v &\approx T_v[D_c] + T_v[D_v] + T_v[T_v] + \\ &T_v[D_c \otimes D_v] + T_v[D_c \otimes D_c] + T_v[S_v \otimes D_c], \end{aligned}$$

with the discarded terms of higher order in  $G$ . Our approximation subsumes the entire set of *fourth* order diagrams for  $\delta E_v$ . This is a substantial improvement over both the SD and the CCSD method which are complete only through the *second* order of MBPT.

Solution of the CCSDvT equations provides us with the wavefunctions and the correlation energies. With the obtained wavefunctions we compute the matrix elements. The relevant CCSDvT formalism is presented in Refs. [10, 11]. In addition to the well-explored SD contributions [5], our formalism includes contributions from the valence triples and also “dressing” of matrix elements. The dressing arises from re-summing nonlinear contributions to the atomic wavefunctions (2) in expressions for matrix elements and, in particular, guarantees that the important chain of random-phase-approximation diagrams is fully recovered in all orders of MBPT [11]. In addition we incorporated all contributions that are quadratic in valence triples. Overall the calculations of matrix elements are complete through the *fifth* order of MBPT and incorporate certain classes of diagrams summed to all orders.

Our numerical calculations are based on our previous CCSDvT code [10], with the addition of the entire set of the non-linear CCSD contributions documented in Ref. [8]. The important new additions are the effects of triples on triples  $T_v[T_v]$  and the leading-order non-linear terms on the r.h.s. of the triples equations. We also employed efficient dual-kinetic-balance basis sets, as described in Ref. [12]. The basis set included partial waves

$\ell = 0-6$  for the S and D amplitudes and  $\ell = 0-4$  for the  $T_v$  amplitudes. Our final results include extrapolation for an infinitely large basis. Since the hyperfine interaction occurs at small distances, due to the uncertainty relation, one has to keep orbitals with high excitation energies in the basis.

TABLE I: Contributions to removal energies of  $2s$ ,  $2p_{1/2}$ , and  $2p_{3/2}$  states for  $^7\text{Li}$  in  $\text{cm}^{-1}$  in various approximations.

	$2s_{1/2}$	$2p_{1/2}$	$2p_{3/2}$
DHF	43087.3	28232.9	28232.3
$\Delta\text{SD}$	405.8	352.0	351.9
$\Delta\text{CCSD}$	-6.8	-5.0	-5.0
$\Delta(T_v[D_v + D_c])^a$	2.8	2.6	2.6
$\Delta(T_v[T_v])$	2.8	3.3	3.3
$\Delta(T_v[\text{NL}])^a$	-1.1	-1.1	-1.1
corrections <sup>b</sup>	-3.3(5)	-0.7(5)	-0.4(5)
Total	43487.5	28584.1	28583.7
Experiment [13]	43487.2	28583.5	28583.2
Other CC works			
SD+MBPT-III [6]	43487.5	28581.9	28581.5
CCSD [14]	43483	28567	

$$^a T_v[D_v + D_c] = T_v[D_v] + T_v[D_c],$$

$$T_v[\text{NL}] = T_v[D_c \otimes D_v] + T_v[D_c \otimes D_c] + T_v[S_v \otimes D_c]$$

<sup>b</sup>includes basis set, recoil, Breit, and QED corrections. Error bar is due to basis extrapolation

TABLE II: Contributions to the magnetic-dipole hyperfine structure constants  $A$  of  $2s$ ,  $2p_{1/2}$ , and  $2p_{3/2}$  states for  $^7\text{Li}$  ( $I = 3/2$ ,  $\mu = 3.256427(2)$ ) in MHz in various approximations.

	$2s_{1/2}$	$2p_{1/2}$	$2p_{3/2}$
DHF	284.35	32.295	6.457
$\Delta\text{SD}$	117.68	13.622	-9.474
$\Delta\text{CCSD}$	-1.79	-0.233	0.176
$\Delta$ dressing	-0.40	-0.039	0.031
$\Delta(T_v[D_v + D_c])$	1.25	0.218	-0.175
$\Delta(T_v[T_v])$	0.28	0.058	-0.031
$\Delta(T_v[\text{NL}])$	-0.04	-0.010	0.002
corrections <sup>a</sup>	0.33(3)	0.046(6)	-0.026(1)
Total	401.66	45.958	-3.041
Experiment	401.75.. <sup>b</sup>	45.914(25) <sup>c</sup>	-3.055(14) <sup>c</sup>
Experiment		46.010(25) <sup>d</sup>	

<sup>a</sup>includes basis set, recoil, Breit, and QED corrections. Error bar is due to the basis extrapolation.

<sup>b</sup>401.7520433(5) Schlecht and McColm [15]; <sup>c</sup>Orth et al. [16]

<sup>d</sup>Walls et al. [17];

In Tables I and II we present calculated energies and magnetic-dipole hyperfine structure (HFS) constants  $A$ . In these tables the entries are ordered by increasing MBPT complexity of the calculations.  $\Delta$  denotes a difference from the preceding entry due to extra classes of the diagrams included at that level of approximation. For example, the entry  $\Delta\text{CCSD}$  is obtained by taking a difference between the CCSD and the SD results. We include Breit, QED, and recoil corrections in our final

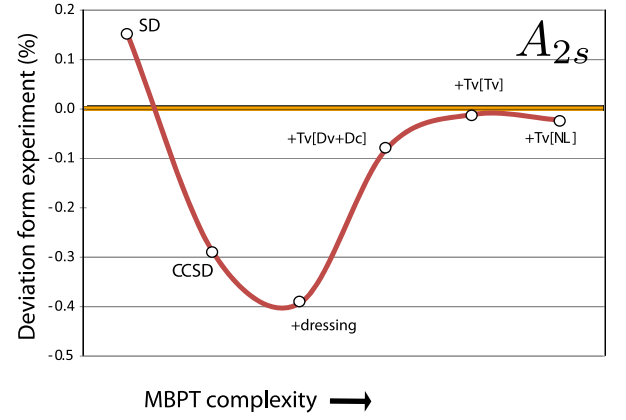


FIG. 2: (Color online) Convergence pattern of the CCSDvT method as a function of MBPT complexity for the HFS constant of the ground state of Li. Breit, QED, recoil and basis set corrections are included in all theoretical values.

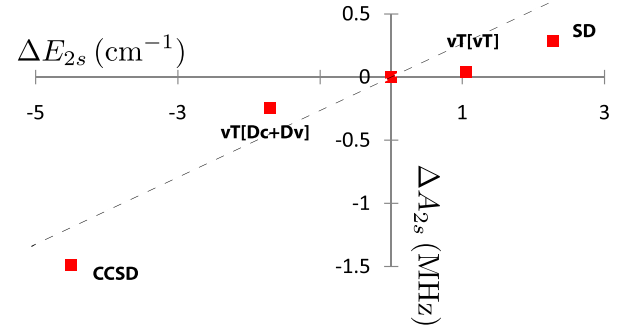


FIG. 3: (Color online) Variations from the final CCSDvT values of  $A_{2s}$  and  $E_{2s}$  in different approximations, e.g.,  $\Delta X_{SD} = X_{SD} - X_{\text{CCSDvT}}$ . The variations in matrix elements and energies are correlated and exhibit linear dependence.

result. For energies they were adopted from Ref. [6], for  $A_{2s}$  from [18], and for  $A_{2p_j}$  from [19]. The basis set extrapolation was carried out in the conventional manner (see, e.g., [6]). The error bar is estimated as a half of the basis-set extrapolation correction. The HFS constants were computed using finite nucleus and uniform magnetization.

The correlation contributions follow a similar pattern in all these cases. We illustrate the convergence of the all-order method in the case of the HFS constant for the ground state in Fig. 2. Here the experimental uncertainty is about 1 ppb so that the deviation from the experimental value is an indication of the theoretical accuracy. The dominant correlations are recovered at the SD level, which captures all third-order diagrams and results in a 0.2% theoretical accuracy. The inclusion of the CCSD non-linear effects and the dressing leads to a worse agreement with the experiment (-0.4%). An inclusion of the leading valence triples returns the agreement to the 0.1% level. The addition of the higher-order  $T_v[T_v]$  effect

results in an almost perfect agreement with the experiment. Finally,  $T_v[\text{NL}]$  diagrams provide only a minor correction. The final result is complete through the fifth order and agrees with the experiment at the 0.02% level.

Finally, we present the computed reduced matrix elements of the electric-dipole operator. We obtain in the CCSDvT approximation with the dressing  $\langle 2s_{1/2} || D || 2p_{1/2} \rangle = 3.31633(7)|e|a_0$  and  $\langle 2s_{1/2} || D || 2p_{3/2} \rangle = 4.6901(1)|e|a_0$ . These values also include basis extrapolation and are complete through the fifth order of MBPT. The error bars here correspond to a half of the basis extrapolation correction. Again, the convergence with respect to the addition of higher-order diagrams follows the same pattern as for the HFS constants (Fig. 2) and energies. To facilitate a comparison with the previous high-accuracy variational studies we form the oscillator strength  $f$  for the  $2s - 2p$  transition. Our result,  $f = 0.74686$ , is smaller than the non-relativistic variational value [20] by 0.01%. The size and the sign of the difference is consistent with the expected difference due to relativistic effects.

The accuracy and the completeness of our calculations allow us to make the following observations.

*Accuracy.* The CCSDvT method improves the accuracy over the previous less complete CC-type calculations. For example, for energies the overall agreement stands at a few  $0.1 \text{ cm}^{-1}$  while the SD method is accurate to a few  $\text{cm}^{-1}$ . Similarly, there is an order of magnitude improvement in the accuracy of computing  $A_{2s}$  over that of the SD approximation. The remaining differences with the experiment are likely due to higher-order diagrams discarded in our scheme; these are consistent with the size of the  $T_v[\text{NL}]$  effect.

*Convergence.* In the absence of general theorems on convergence of MBPT, the present work provides an empirical proof that the CC method converges for Li. For

all the computed properties the saturation of the method with respect to adding increasingly complex classes of diagrams is not monotonic, as illustrated in Fig. 2. The empirical conclusion for other, more complex, univalent atoms is that both the non-linear CCSD effects and the valence triples have to be treated simultaneously [2].

*Correlation between corrections to the energy and to the matrix elements.* There is a strong link between the convergence patterns for energies and for matrix elements. This is illustrated in Fig. 3: the deviations of the  $A_{2s}$  and  $E_{2s}$  from the final CCSDvT values follow roughly a linear law. The data for matrix elements does not include dressing. A similar pattern is observed for other matrix elements as well. Such a linear dependence is due to the effect of self-energy (Brueckner) correction. This dominant chain of diagrams is presented in both matrix elements and energies. For example, for triple excitations, the corrections  $S_v[T_v]$  and  $\delta E_v[T_v]$  arise from the same diagram and the modification of singles due to triples propagates into the calculation of the matrix element. Similar scaling ideas were used earlier [3, 4] to fit low-order results to higher orders, but never rigorously tested. Of course, as apparent from Fig. 3, the linear scaling is only approximate and can be used in the semi-empirical fits only to a certain accuracy. For example, the self-energy corrections do not affect “dressing” of matrix elements which contributes at a sizable 0.1% level to the  $A_{2s}$  constant. Neither can it capture the distinctively-different QED corrections to the energies and matrix elements.

We would like to thank V. Dzuba and V. Yerokhin for discussions. This work was supported in part by the National Science Foundation. S.G.P. was supported in part by the RFBR under grants No. 07-02-00210-a and 08-02-00460-a.

- 
- [1] M. L. Leininger, W. D. Allen, H. F. Schaefer III, and C. D. Sherrill, *J. Chem. Phys.* **112**, 9213 (2000).
  - [2] A. Derevianko and S. G. Porsev, *Eur. Phys. J. A* **32**, 517 (2007).
  - [3] V. Dzuba, V. Flambaum, and J. Ginges, *Phys. Rev. D* **66**, 076013/1 (2002).
  - [4] W. R. Johnson, Z. W. Liu, and J. Sapirstein, *At. Data Nucl. Data Tables* **64**, 279 (1996).
  - [5] S. A. Blundell, W. R. Johnson, Z. W. Liu, and J. Sapirstein, *Phys. Rev. A* **40**, 2233 (1989).
  - [6] W. R. Johnson, U. I. Safronova, A. Derevianko, and M. S. Safronova, *Phys. Rev. A* **77**, 022510 (2008).
  - [7] I. Lindgren and J. Morrison, *Atomic Many-Body Theory* (Springer-Verlag, Berlin, 1986), 2nd ed.
  - [8] R. Pal, M. S. Safronova, W. R. Johnson, A. Derevianko, and S. G. Porsev, *Phys. Rev. A* **75**, 042515 (2007).
  - [9] A. Derevianko and E. D. Emmons, *Phys. Rev. A* **66**, 012503 (2002).
  - [10] S. G. Porsev and A. Derevianko, *Phys. Rev. A* **73**, 012501 (2006).
  - [11] A. Derevianko and S. G. Porsev, *Phys. Rev. A* **71**, 032509 (2005).
  - [12] K. Beloy and A. Derevianko, *Comp. Phys. Comm.* (2008), doi:10.1016/j.cpc.2008.03.004.
  - [13] Y. Ralchenko, A. E. Kramida, J. Reader, and NIST ASD Team, *NIST atomic spectra database (version 3.1.4)* (2008), URL <http://physics.nist.gov/asd3>.
  - [14] E. Eliav, U. Kaldor, and Y. Ishikawa, *Phys. Rev. A* **50**, 1121 (1994).
  - [15] R. G. Schlecht and D. W. McColm, *Phys. Rev.* **142**, 11 (1966).
  - [16] H. Orth, H. Ackermann, and E. W. Otten, *Z. Phys. A* **273**, 221 (1975).
  - [17] J. Walls, R. Ashby, J. Clarke, B. Lu, and W. A. van Wijngaarden, *Eur. Phys. J. D* **22**, 159 (2003).
  - [18] V. A. Yerokhin, *Phys. Rev. A* **77**, 020501 (2008).
  - [19] J. Bieroń, P. Jönsson, and C. Froese Fischer, *Phys. Rev. A* **53**, 2181 (1996).
  - [20] Z.-C. Yan and G. W. F. Drake, *Phys. Rev. A* **52**, 3711 (1995).